Submitted to: phys. stat. solidi

Current spreading, heat transfer, and light extraction in multi-pixel LED array

M. V. Bogdanov[1], K. A. Bulashevich[1,2], I. Yu. Evstratov[1], and S. Yu. Karpov[3] *

[1] Soft-Impact, Ltd., P.O. Box 83, St.Petersburg, 194156 Russia
[2] Ioffe Physico-Technical Institute RAS, 26 Polytechnicheskaya, St.Petersburg, 194021 Russia
[3] STR, Inc., P.O. Box 70604, Richmond, VA 23255-0604, USA

Received …, accepted …
Published online …

PACS 85.60.Jb, 85.60.Bt, 44.90.+c

Using simulation, we have investigated into the current spreading, heat transfer, and light emission in a high-power light-emitting diode (LED) with an interdigitated multipixel array (IMPA) chip design. The main advantages of such LEDs compared with conventional square-shaped ones, like a lower series resistance and a higher emission efficiency at high currents, are interpreted in terms of current spreading and local active region overheating originated from the current crowding typical for planar LED dice.

Preprint 2007

1 Introduction Generally, III-nitride light-emitting diodes (LEDs) fabricated on sapphire substrates suffer from the current crowding [1-3] and subsequent active region overheating [4], eventually resulting in a reduction of the light emission efficiency at high operation currents. In order to improve the high-current LED performance, an interdigitated multipixel array (IMPA) chip design has been recently suggested in [5], primarily aimed at the current crowding suppression.

In this paper we report on the simulation study of the IMPA LED with the focus on advantages provided by the novel chip design. We consider coupled current spreading, heat transfer, and light extraction in the IMPA and conventional square-shaped LED dice to get a deeper insight into specific features of their operation. The theoretical predictions are compared with the data reported in [5].

2 Results Following [5], we compare here the IMPA die consisting of a hundred of 30×30 μm^2 pixel-LEDs integrated on a sapphire substrate with a conventional square-shaped 300×300 μm^2 LED die. The LED heterostructure employed in both dice and the IMPA design have been discussed in detail in [5]. As the square chip was not described in [5], we have chosen rather arbitrary but typical electrode configuration shown in Fig.2. Both dice had the same light emitting area, while the total area of the IMPA LED is about an order of magnitude larger than that of the square one. The output optical power of the LEDs was measured in [5] by collecting the light extracted through the back side of the sapphire substrate. The *n*- and *p*-contact resistances were 5×10^{-5} Ω·cm^2 and 1×10^{-3} Ω·cm^2, respectively, in accordance with data reported in [5]. The LED heterostructure provided the emission spectrum peaked at 400 nm.

To investigate into the device operation, we used the SimuLED package [6] that provides coupled analysis of the current spreading, heat transfer, and light extraction in the LED dice. The hybrid approach underlying the simulation has been briefly discussed in [7]. It includes 1D modelling of the LED heterostructure coupled with 3D simulation of the current spreading and heat transfer in the die. 3D ray tracing is used to analyze the light propagation inside the die and its extraction to outside.

The computed band diagram of the Ga-polar LED heterostructure and the partial electron and hole current densities corresponding to the total current density j = 160 A/cm^2 are shown in Fig.1. One can see that the conduction and valence bands in the *p*- and *n*-GaN contact layers, as well as in the *n*-GaN

* Corresponding author: e-mail: karpov@semitech.us, Phone: +1 (804) 615 0038, Fax: +1 (804) 639 7114

barriers separating individual InGaN quantum wells, are nearly flat at such a current density. The electric field remains unscreened only in the *p*-AlGaN blocking layer, quantum wells, and narrow space-charge regions adjacent to the wells.

The distributions of the electron and hole current densities show that electrons can easily penetrate through the multiple-quantum-well active region, partly leaking into the *p*-GaN contact layer. The simulation predicts about 7% of electrons to be lost at the *p*-electrode because of leakage at j = 160 A/cm^2. At a higher current density or at an elevated temperature, the electron leakage becomes much more pronounced, considerably reducing the internal quantum efficiency of the LED structure.

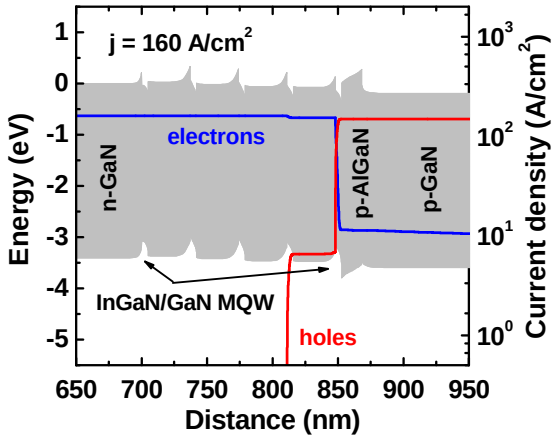

Fig.1 Computed room-temperature band diagram and partial electron and hole current densities in the violet LED hetero-structure reported in [5]. The bandgap is marked by grey shadow.

The partial hole current density becomes negligibly small when holes pass through the quantum well adjacent to the *p*-AlGaN blocking layer. As a result, only this well is filled sufficiently with holes, giving the major rise to the radiative carrier recombination. Actually, just this well serves as an efficient light emitter, providing more than 95% of emitted photons, while other quantum wells operate under non-optimal conditions.

Fig.2 (top) displays the predicted current density distribution over the active region of square LED at the forward current of 50 mA. One can see that current crowding is mainly observed near the gap between the *n*- and *p*-contact electrodes. The current density varies about three times at 50 mA and about six times at 300 mA in the cross section marked in Fig.2. The variation is found to be nearly exponential with a specific decay or current-spreading length L of ~80 μm at 50 mA and ~70 μm at 500 mA. The current-spreading length found in this study is about 3 times smaller than that derived in [5] on the basis of analytical estimates. Such a big discrepancy between the two values of the current-spreading length shows that the analytical estimates may be inadequate because of ignoring the interrelation between the current localization area and electric potential distribution inside the LED die. This interrelation leads, in particular, to the dependence of the current spreading length on the current through the diode, which is an evidence for a non-linear character of the current crowding.

The heat transfer in the die is simulated, assuming the heat sinking through the back side of the sapphire substrate. The temperature distributions in the selected cross section corresponding to different forward currents are plotted in Fig.2 (bottom). The temperature rises near the interelectrode gap by ~150 K at 300 mA and by ~350 K at 500 mA, while the mean temperature of the active region exceeds the room temperature by only 55 K and 120 K at these currents, respectively. As a result of the overheating, the output optical power of the square LED starts to saturate at the forward currents as high as 400 mA. At higher currents, the optical power rollover is predicted to occur, which is in close agreement with observations (see Fig.3).

Simulation of the IMPA LED has demonstrated extremely high uniformity of the current density and temperature in the active region. This is largely due to the choice of the pixel dimensions to be a few

times less than the current spreading length in the conventional LED. The difference in the current density between the pixels located in the centre and on the periphery of the IMPA die is less than ~0.5% at the forward current as high as 3.5 A. In turn, the respective temperature difference does not exceed 6% at such a high operation current. The predicted maximum overheating of the active region is about 20 K at 500 mA and about 260 K at 3.5 A, respectively. The remarkably lower overheating of the IMPA LED is primarily due to its extended chip area. The uniform current density and temperature distributions in the IMPA LED provide a small scatter of the emission wavelength and electroluminescence (EL) intensity between different pixels. This conclusion is in line with the observations made in [5].

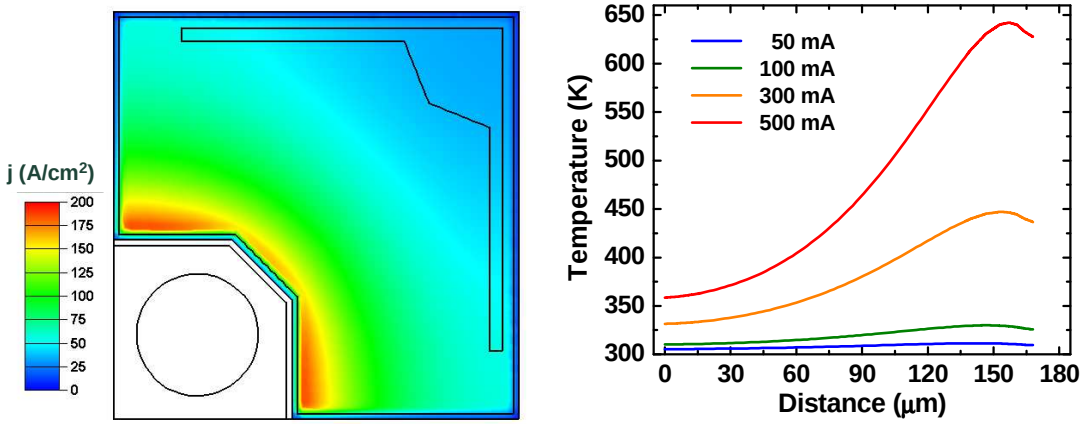

Fig. 2 Two-dimensional distributions of the current density in the active region of square LED at 50 mA (top) and temperature profiles in the selected cross section at different currents (bottom). The distance is counted from the die edge.

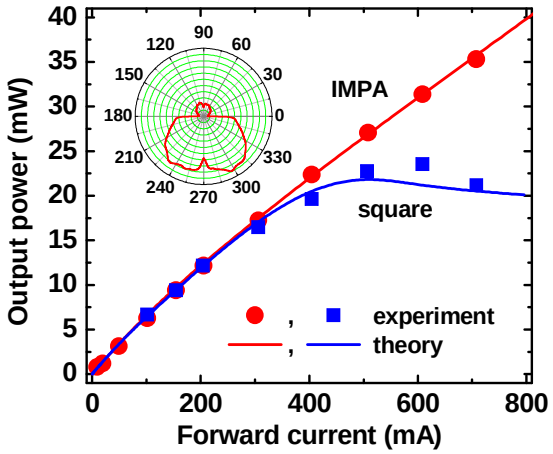

Fig. 3 Theoretical and experimental output optical power of the IMPA and square LEDs as a function of operation current. Inset shows the far-field emission pattern that is nearly the same for the IMPA and square LEDs.

The lower overheating and much more uniform current density distribution in the active region provide the output optical power to grow with current without rollover up to 3.5 A. Some tendency to the output power saturation is predicted only for the currents higher than 3.0 A. This means that the IMPA LED is capable of high-current operation, in contrast to the square LED.

Our simulations predict the series resistance of 1.2 Ω for the IMPA LED and about 7-9 Ω for the square LED, respectively. The theoretical values agree well with the series resistances of 1.0 Ω and 8 Ω

reported in [5]. In order to understand this result, one can estimate roughly the series resistance as $R \approx (L/\sigma dp)^{-1}$, where σ is the electric conductivity of the *n*-contact layer, d is *n*-contact layer thickness under the *n*-electrode, and p is the electrode perimeter, through which the current effectively flows. At d = 1.7 μm and p = 240 μm, the estimate provides the series resistance of ~7 Ω for square LED, in good agreement with simulation and experiment. In the case of the IMPA LED, the current spreading length L should be taken equal to the side length of an individual pixel, i.e. to 30 μm. Then at p = 1800 μm (the length of a *p*-pad multiplied by the number of pixels), the estimated series resistance is about 0.4 Ω, which is three times lower than the value obtained by direct simulation. The discrepancy may be addressed to the contribution of the *p*-contact layer resistance that was neglected in the above rough estimate. Nevertheless, it shows that the series resistance is primarily controlled by the electrode perimeter which is much larger for the IMPA LED.

We have found a discrepancy between the computed (~3.2-3.3 V) and measured (~3.7-3.8 V) turn-on voltages of the square and IMPA LEDs. As the former value is close to those repeatedly reported for blue and violet LEDs in other papers, we attribute the discrepancy between the theoretical and experimental turn-on voltage to the non-ohmic behaviour of the *p*-contact, which is not accounted for in the simulations.

The total light extraction efficiency is found to be ~15% for both dice, independently of current. To explain rather low values of the measured external quantum efficiencies of both types of LED, we had to suppose a strong light absorption inside the dice, presumably occurring in the *p*-GaN contact layer. Only ~3% of all emitted photons is predicted to be extracted through the semitransparent *p*-electrode (see the inset in Fig.3). The rest 12% of photons leaves the dice through the side walls and back side of the sapphire substrate.

3 Conclusion Using simulations, we have analyzed specific features of the IMPA LED operation, in comparison with an LED of conventional square-shape design. Due to suppressed current crowding and more tranquil thermal operation conditions, the IMPA LED can serve as a high-brightness light source, working without rollover of the optical power and having a low series resistance. High uniformity of the current density and temperature in the active region provides excellent emission wavelength uniformity over the extended IMPA die.

We used in the study an approximate hybrid approach that has been found to give the results close to available observations. The approach enables coupled modelling of the current spreading and heat transfer in an LED die of a complex geometry. Since the interplay between the thermal and current-spreading effects is an important factor that affects the LED operation, considering them self-consistently is quite critical for adequate simulation of the light-emitting devices utilizing an elaborated design.

Acknowledgements The work of K.A. Bulashevich was supported in part by the Russian Federal Program on Support of Leading Scientific Schools and Russian Foundation for Basic Research (grant 05-02-16679).

References

[1] I. Eliashevich, Y. Li, A. Osinsky, C. A. Tran, M. G. Brown, and R. F. Karlicek, Jr., Proc. SPIE **3621**, 29 (1999).
[2] H. Kim, J.-M. Lee, C. Huh, S.-W. Kim, D.-J. Kim, S.-J. Park, and H. Hwang, Appl. Phys. Lett. **77**, 1903 (2000).
[3] X. Guo and E. F. Schubert, Appl. Phys. Lett. **78**, 3337 (2001).
[4] K. A. Bulashevich, I. Yu. Evstratov, V. F. Mymrin, and S. Yu. Karpov, phys. stat. sol. (c) **4**, 45 (2007).
[5] A. Chakraborty, L. Shen, H. Masui, S. P. DenBaars, and U. Mishra, Appl. Phys. Lett. **88**, 181120 (2006).
[6] http://www.semitech.us/products/
[7] I. Yu. Evstratov, V. F. Mymrin, S. Yu. Karpov, and Yu. N. Makarov, phys. stat. sol. (c) **3**, 1645 (2006).
[4] M. E. Levinshtein, S. L. Rumyantsev, and M. S. Shur (eds), Properties of advanced semiconductor materials. GaN, AlN, InN, BN, SiC, SiGe., (Wiley-Interscience, New York, 2001), p.9-11.
[5] http://www.semitech.us/products/
[6] S. Yu. Karpov, K. A. Bulashevich, I. A. Zhmakin, M. O. Nestoklon, V. F. Mymrin, and Yu. N. Makarov, Phys. Stat. Solidi (b) **241**, 2668 (2004).
[7] X. A. Cao and S. D. Arthur, Appl. Phys. Lett. **85**, 3971 (2004).